

## Chapter 2

# Monitoring and Checking of Performance in Photovoltaic Plants

This chapter presents the results of the study conducted in the framework of the European Project PERSIL, published in the paper [30]. The work represented the Photovoltaic section of the European Project PERSIL, which included also the study of solar thermal plants. The activity was twofold: the results of 1-year monitoring and checking of thirteen PV systems; the consequent guidelines for the design, installation and maintenance of grid connected PV systems. For accurate estimation of the energy production a two-year analysis of solar radiation was conducted on the basis of pyranometer measurements in all the Project locations. The checking of energy performance was carried out by a suitable improvement of a conventional method, that included the assessment of the energy availability. The corresponding results were excellent for three PV plants, whereas they are strongly negative for five old PV plants which exhibit poor availability (62–78%). The remaining plants behave with acceptable performance ratios (0.65–0.78). This work well presents which kind of issues can have the some BIPV systems in an urban environment respect to others, ground-mounted or not, with less problems, including a long term assessment of the energy production compared to a theoretical production potential.

## 2.1 PERSIL project

In the recent past, in Germany, Italy and France various feed-in tariffs were available for PhotoVoltaic (PV) systems and the maximization of productivity was of paramount importance. This goal can be achieved by many solutions, as discussed in the paper [3]. The PERSIL (Solar Performance and Local Industry) [31] was an European project which involved public and industrial organizations in Italy, Environment Park, Province of Turin, Turin Industry Association, and in France, Departments of Savoie and Hautes-Alpes. This project (2009-2011) was thought to achieve the following goals:

- to collect performance data on Solar Thermal and PV plants installed in the local area;
- to enhance the technology transfer among the two Countries;
- to promote the technology innovation through the creation of test sites from the solar technology viewpoint;
- finally, more in general, to boost the collaboration between Research Centres and Industry.

In this framework the “Politecnico di Torino” University was called by the Province of Turin to perform the monitoring activity of thirteen different PV plants installed in its territory [32], during one year period, and, at the conclusion, to define the reference guidelines for the PV designers, installers, Operation and Maintenance (O&M) workers [33]. The PV plants were mainly installed on public schools, but also a test facility, an apartment block, a climbing centre and an industrial site were taken into account. The choice criteria were, obviously, accurate measurements from data-logger, different PV module technology, rated power and kind of installation. In the following a study of the two-year radiation in the project locations and the results of monitoring/checking of the thirteen PV systems with the assessment of the energy availability are discussed.

## 2.2 2009–2010 Radiation in Project Locations

Due to the tutorial goal for designers and installers in area of Province of Turin, updated irradiation data from a wide number of locations have been collected and processed, since the previously available data were 20-year old. Within the period 2009–2010, ten meteorological stations of the local Agency for Environmental Protection (ARPA-Piedmont), equipped with pyranometers for the measurement of the horizontal global irradiation, have been considered from the viewpoint of the energy production in the Province of Turin. Its corresponding surface is about 6800 km<sup>2</sup> with maximum distances among the locations of less than 100 km: the distribution of the 10 sites (Fig. 2.1), hence, is representative of the climatology in the Province of Turin. The measurements, performed on the horizontal plane, have been transferred on a tilted plane typical for the building integration (pitched roof towards South with 25° angle). The procedure for the data correction can be carried out by multiple methods, as for example the one proposed in the Italian standard [34] or in other documents [35]. The selected weather stations have been installed in different locations, starting from two in the city of Turin “Via Consolata” (downtown, altitude 290 m a.s.l.) and “Via Reiss Romoli” (outskirts, 270 m a.s.l.). In the peripheral zone three stations have been considered: Avigliana (340 m a.s.l.) towards West; Pino Torinese (600 m a.s.l.) towards East; Bauducchi (230 m a.s.l.) towards South. Far from Turin, in the Western territory of “Susa Valley” two stations have been chosen: Bardonecchia (location Pranudin 2000 m a.s.l.) on a mountain; Borgone at a lower altitude (400 m a.s.l.). Far from Turin, in the Northern “Canavese” zone, two other stations have been included: Caselle (300 m a.s.l.) and Candia (230 m a.s.l.). Finally, the station of Carmagnola (230 m a.s.l.) has been considered as representative of the Southern zone of the Province of Turin.

From the readings of the 2009-2010 data (Table reported in Fig. 2.2), it is clear that the year 2010 for the radiation has been less profitable than the year 2009, in fact eight out of the ten sites exhibit reductions within 5%–9% with higher frequency in the range of 6%–7%. Only in the stations of Carmagnola and Turin (downtown) the variations are negligible or within the uncertainty of measurements ( $\pm 3\%$ ). The remarkable reduction of radiation in 2010 is essentially

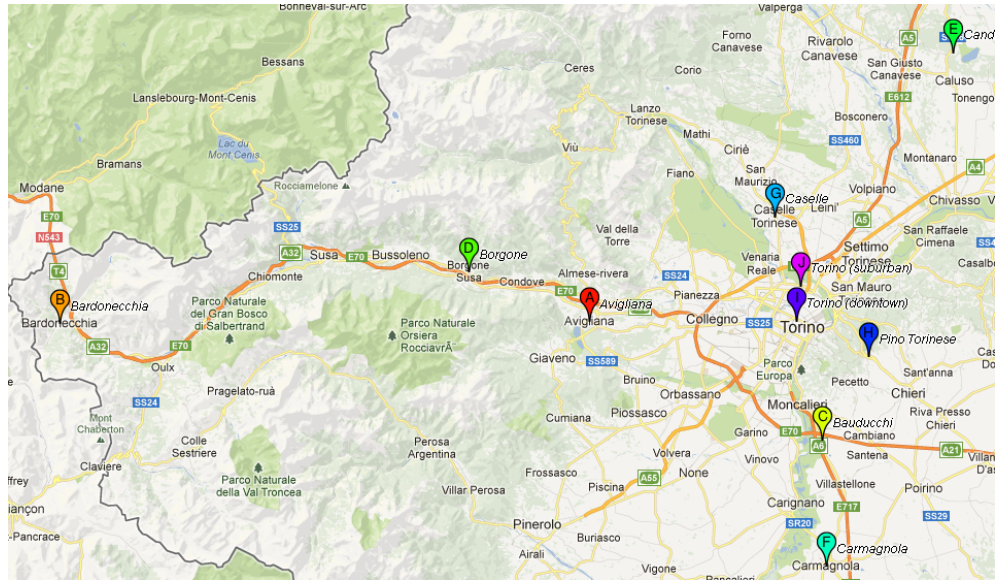


Figure 2.1: Locations of the 10 ARPA — Piedmont meteorological stations.

concentrated in February, May, June and October with variations up to 30%. It is worth noting that in 2010 the more impressive decrements in  $\text{kWh/m}^2$  are in May and June, while if the percentage decreases are considered, they are found in February and October. Obviously, among the two types of decrements, the most important ones from the productivity viewpoint are those expressed in  $\text{kWh/m}^2$ . On the other hand, in all the meteorological stations a huge increment has been recorded in April with variations always higher than 30% on the tilted plane. As could be expected due to the remarkable altitude without important obstructions, the station of Bardonecchia has been characterized by the best radiation (above  $1550 \text{ kWh/m}^2$  on the horizontal plane and about  $1850 \text{ kWh/m}^2$  on the selected tilted plane in 2009). However, the site of the lower Susa valley (Borgone) has been limited by the shades generated by the surrounding mountains and has a poor ranking. Also the stations of Caselle, Pino Torinese e Bauducchi in the year 2009 show particularly favourable results for the horizontal radiation per annum (above  $1400 \text{ kWh/m}^2$ ): if this value is transferred to the tilted plane of  $25^\circ$  towards South, the radiation exceeds  $1600 \text{ kWh/m}^2$ . In the station Bauducchi the figures of radiation both on the horizontal and tilted planes are very similar to the

station Pino Torinese (explained by the geographical closeness). The Carmagnola station exhibits a very particular climate, since with the same value in the two-year period the radiation of 2009 yields the number nine and the radiation of 2010 achieves the second place in the ranking. If we examine the two stations of city of Turin (Via Consolata and Via Reiss Romoli), the most important thing is that in 2009 the station located in outskirts (Reiss Romoli) show a higher radiation than the downtown station (Consolata), whereas in 2010 the values of radiation are practically equivalent and quite reduced. In particular, in 2009 the measurements on the horizontal plane provide above  $1350 \text{ kWh/m}^2$  in outskirts and below  $1300 \text{ kWh/m}^2$  in downtown, but in 2010 both the stations give a value around  $1270 \text{ kWh/m}^2$ . Therefore, the radiation in the downtown station does not substantially change, due to the air pollution that scatters the direct radiation and increase the diffuse radiation. Finally, one can claim that Bardonecchia is the site with the best irradiation and the station in downtown Turin takes the last place, in this case the gain with respect to the worst site exceeds 20%. If we omit the mountain site, however, the better locations (Caselle, Pino Torinese e Bauducchi) yield a gain of about 10% with reference to downtown Turin.

ID	Location	2009		2010		$\Delta H_{\text{hor}}$ ( $\text{kWh/m}^2$ )	$\Delta H_{\text{tilted}}$ ( $\text{kWh/m}^2$ )	$\epsilon_{\text{H hor}}$	$\epsilon_{\text{H tilted}}$
		$H_{\text{hor}}$ ( $\text{kWh/m}^2$ )	$H_{\text{tilted}}$ ( $\text{kWh/m}^2$ )	$H_{\text{hor}}$ ( $\text{kWh/m}^2$ )	$H_{\text{tilted}}$ ( $\text{kWh/m}^2$ )				
A	Avigliana	1398	1604	1319	1491	-80	-113	-6%	-7%
B	Bardonecchia	1573	1845	1493	1726	-80	-119	-5%	-6%
C	Bauducchi	1425	1593	1340	1474	-85	-118	-6%	-7%
D	Borgone	1382	1575	1309	1471	-73	-104	-5%	-7%
E	Candia	1399	1580	1306	1462	-92	-119	-7%	-8%
F	Carmagnola	1378	1526	1378	1524	0	-2	0%	0%
G	Caselle	1445	1637	1350	1508	-96	-129	-7%	-8%
H	Pino Torinese	1435	1637	1329	1487	-106	-150	-7%	-9%
I	Torino (downtown)	1300	1470	1277	1430	-23	-40	-2%	-3%
J	Torino (suburban)	1369	1544	1278	1422	-92	-123	-7%	-8%

Figure 2.2: Solar Irradiance Data for Project Locations in 2009 and 2010 Years.

The table in Fig. 2.3 sums up the irradiation data for Turin (urban in downtown and outskirts), Pino Torinese (suburban) and Avigliana (country environment), needed for the further monitoring activity after the correction procedure,

Avigliana	2009		2010		$\Delta H_{hor}$ (kWh/m <sup>2</sup> )	$\Delta H_{tilted}$ (kWh/m <sup>2</sup> )	$\epsilon_H_{hor}$	$\epsilon_H_{tilted}$
	H <sub>hor</sub> (kWh/m <sup>2</sup> )	H <sub>tilted</sub> (kWh/m <sup>2</sup> )	H <sub>hor</sub> (kWh/m <sup>2</sup> )	H <sub>tilted</sub> (kWh/m <sup>2</sup> )				
Jan	1.70	2.86	1.37	2.16	-0.33	-0.70	-19%	-25%
Feb	2.80	4.16	2.15	2.98	-0.65	-1.17	-23%	-28%
Mar	3.67	4.56	3.06	3.67	-0.62	-0.88	-17%	-19%
Apr	3.66	3.88	4.81	5.20	1.15	1.33	31%	34%
May	5.91	5.88	5.01	4.96	-0.90	-0.91	-15%	-16%
Jun	6.71	6.43	5.58	5.36	-1.13	-1.08	-17%	-17%
Jul	6.37	6.21	6.46	6.30	0.09	0.09	1%	1%
Aug	5.48	5.74	5.43	5.68	-0.05	-0.06	-1%	-1%
Sep	3.87	4.50	4.15	4.87	0.28	0.37	7%	8%
Oct	2.89	3.96	2.34	3.07	-0.54	-0.89	-19%	-23%
Nov	1.57	2.40	1.55	2.36	-0.02	-0.03	-1%	-1%
Dec	1.26	2.12	1.35	2.33	0.09	0.21	7%	10%

Pino Torinese	2009		2010		$\Delta H_{hor}$ (kWh/m <sup>2</sup> )	$\Delta H_{tilted}$ (kWh/m <sup>2</sup> )	$\epsilon_H_{hor}$	$\epsilon_H_{tilted}$
	H <sub>hor</sub> (kWh/m <sup>2</sup> )	H <sub>tilted</sub> (kWh/m <sup>2</sup> )	H <sub>hor</sub> (kWh/m <sup>2</sup> )	H <sub>tilted</sub> (kWh/m <sup>2</sup> )				
Jan	1.67	2.80	1.30	2.01	-0.37	-0.79	-22%	-28%
Feb	2.88	4.31	2.17	3.01	-0.71	-1.30	-25%	-30%
Mar	3.76	4.69	3.11	3.75	-0.65	-0.94	-17%	-20%
Apr	3.79	4.02	4.83	5.24	1.05	1.21	28%	30%
May	6.24	6.22	5.09	5.05	-1.15	-1.17	-18%	-19%
Jun	6.97	6.68	5.96	5.72	-1.01	-0.96	-14%	-14%
Jul	6.64	6.48	6.74	6.57	0.10	0.10	1%	2%
Aug	5.65	5.93	5.50	5.76	-0.15	-0.17	-3%	-3%
Sep	4.06	4.75	4.08	4.78	0.02	0.02	0%	1%
Oct	2.84	3.88	2.22	2.88	-0.62	-1.00	-22%	-26%
Nov	1.32	1.93	1.29	1.86	-0.04	-0.07	-3%	-4%
Dec	1.25	2.10	1.31	2.22	0.05	0.12	4%	6%

Turin, suburban	2009		2010		$\Delta H_{hor}$ (kWh/m <sup>2</sup> )	$\Delta H_{tilted}$ (kWh/m <sup>2</sup> )	$\epsilon_H_{hor}$	$\epsilon_H_{tilted}$
	H <sub>hor</sub> (kWh/m <sup>2</sup> )	H <sub>tilted</sub> (kWh/m <sup>2</sup> )	H <sub>hor</sub> (kWh/m <sup>2</sup> )	H <sub>tilted</sub> (kWh/m <sup>2</sup> )				
Jan	1.44	2.30	1.14	1.71	-0.30	-0.59	-21%	-26%
Feb	2.50	3.60	2.00	2.73	-0.50	-0.87	-20%	-24%
Mar	3.59	4.44	3.07	3.70	-0.52	-0.74	-14%	-17%
Apr	3.74	3.97	4.88	5.29	1.14	1.32	30%	33%
May	5.97	5.94	5.08	5.04	-0.89	-0.90	-15%	-15%
Jun	6.74	6.46	5.59	5.36	-1.15	-1.10	-17%	-17%
Jul	6.35	6.19	6.16	6.00	-0.20	-0.19	-3%	-3%
Aug	5.47	5.72	5.30	5.53	-0.17	-0.19	-3%	-3%
Sep	3.92	4.56	4.13	4.84	0.21	0.28	5%	6%
Oct	2.72	3.67	2.17	2.79	-0.55	-0.88	-20%	-24%
Nov	1.34	1.96	1.22	1.75	-0.12	-0.21	-9%	-11%
Dec	1.16	1.90	1.18	1.94	0.02	0.04	1%	2%

Turin, downtown	2009		2010		$\Delta H_{hor}$ (kWh/m <sup>2</sup> )	$\Delta H_{tilted}$ (kWh/m <sup>2</sup> )	$\epsilon_H_{hor}$	$\epsilon_H_{tilted}$
	H <sub>hor</sub> (kWh/m <sup>2</sup> )	H <sub>tilted</sub> (kWh/m <sup>2</sup> )	H <sub>hor</sub> (kWh/m <sup>2</sup> )	H <sub>tilted</sub> (kWh/m <sup>2</sup> )				
Jan	1.42	2.26	1.21	1.85	-0.20	-0.41	-14%	-18%
Feb	2.63	3.84	2.02	2.75	-0.61	-1.08	-23%	-28%
Mar	3.37	4.11	3.02	3.62	-0.35	-0.49	-10%	-12%
Apr	3.43	3.61	4.75	5.14	1.32	1.52	39%	42%
May	5.49	5.46	4.90	4.86	-0.59	-0.60	-11%	-11%
Jun	6.10	5.85	5.58	5.36	-0.52	-0.50	-8%	-8%
Jul	6.08	5.92	6.08	5.93	0.01	0.01	0%	0%
Aug	5.22	5.45	5.29	5.52	0.06	0.07	1%	1%
Sep	3.73	4.31	4.15	4.87	0.42	0.55	11%	13%
Oct	2.76	3.75	2.29	2.98	-0.47	-0.77	-17%	-20%
Nov	1.25	1.80	1.31	1.90	0.06	0.10	5%	6%
Dec	1.18	1.94	1.30	2.20	0.12	0.26	10%	14%

Figure 2.3: Details of Average Daily Solar Irradiance Data for the 4 Selected Locations.

according to the sun exposition of the PV systems with respect to the horizontal plane.

## 2.3 Methodology of study

The monitoring activity led to an huge amount of collected data on the produced energy by each PV system. Each monitored data, in terms of daily energy at AC side with accuracy within  $\pm 1\text{--}3\%$ , is compared with a value which represents a production in reference conditions, i.e., assuming 100% availability of the system. In this sense, for example, whenever a PV array composed of  $N_p$  parallel strings is operating with  $(N_p \cdot \check{U}n)$  strings, it has not full availability, lacking the contribution of  $n$  strings. The energy availability [36] depends on several items, such as planned/unplanned maintenance, failures and repairs of the main components (PV modules, cables, inverters and protections) and grid faults. In the past sixteen years the availability was less than 95% and it influences all the lifespan of PV plants (at least 20 years), while in recent years the performance can exceed 99% in the best cases [37]. In case of lacking measurements from the data-loggers, also the reference production and the corresponding comparison have not been considered. The above mentioned estimation of the reference production is computed starting from the Italian standard [2], instead of more complex models [38, 39], with the following formula

$$E_{AC_p} = P_{rated} \cdot Y_r \cdot \eta_{th} \cdot \eta_{array} \cdot \eta_{shade} \cdot \eta_{inv} \quad (2.1)$$

where

$E_{AC_p}$  is the predicted daily energy;

$P_{rated}$  is the power rating of the PV array;

$Y_r$  is the reference yield [1] on the PV plane (from the calibrated pyranometers of the local Agency for Environmental Protection, ARPA-Piedmont);

$\eta_{th}$  takes into account the temperature losses and it is equal to  $(1 + \gamma \Delta T)$ , where

$\gamma$  is the thermal coefficient of the PV module maximum power and  $\Delta T$  is the temperature deviation of the solar cells from the standard value (25 °C);

$\eta_{array}$  represents the non-thermal loss contribution of the PV array, such as DC cables, manufacturing tolerance and I-V mismatch, dirt, reflection, etc. It is fixed at 92% by the Standard [2] for PV modules of recent production (less than four years) characterized by a typical tolerance equal to  $\pm 3\%$  or less, while for older PV modules in this paper it is considered equal to 86%, because of a wider tolerance of  $\pm 5\%$  and higher deposition of pollution;

$\eta_{shade}$  determines the shading effect on the PV array [40, 41], simply computed as ratio of the actual energy output to the available energy without shade, during a sunny day near equinoxes;

$\eta_{inv}$  is a weighted inverter efficiency in function of the power output [26].

This energy prediction is compared with the monitored value  $E_{AC_m}$  (both affected by uncertainty, see [37]) by the relative deviation according to 2.2. Thus, the availability  $A_E$  can be expressed with the formula 2.3

$$\epsilon_{p-m} = \frac{E_{AC_p} - E_{AC_m}}{E_{AC_p}} \quad (2.2)$$

$$A_E = 1 - \epsilon_{p-m} \quad (2.3)$$

For all the PV systems the annual performance is reported in terms of the conventional parameters, reference yield  $Y_r$ , final yield  $Y_f$  and performance ratio  $R_p$  [1, 42]. Table in Fig. 2.13, in which an year of daily monitoring is summarized, shows that the PV plants behave in a very different way. Indeed, three PV plants are excellent, other five ones have poor performance and the remainder is close to the average. It has been decided to give a rank according to different performance ratio ranges. If  $R_p \geq 0.8$ , the rank is “excellent”; in case of  $0.75 \leq R_p \leq 0.79$ , “good”; in case of  $0.70 \leq R_p \leq 0.74$ , “sufficient”; in case of  $0.60 \leq R_p \leq 0.69$ , “mean”; finally, in case of  $R_p \leq 0.59$ , “poor”.



## 2.4 The Thirteen Monitored PV Systems

As previously mentioned, the thirteen monitored PV systems are selected on the basis of the significant interest due to power rating, the site and mode of installation, and the technology of the PV modules. The power rating ranges from a few kilowatt to 250 kW<sub>p</sub>. The sites of installation are mainly three locations (Turin, Avigliana, Pino Torinese) within the Province of Turin, far each other about a few tens of kilometres (45° N latitude). In this way the urban, suburban and country environments are represented. The PV systems are constituted by all fixed installations, but one sub-field of the public school called “E” is mounted on a double axis sun-tracking system. Among the fixed systems only one is totally integrated, being made of solar cells encapsulated in the glass which makes the rooftop of the building. It is the case of the climbing centre. The technologies of the PV modules are the commercial ones: in the most of the cases it is mono-crystalline (m-Si) or poly-crystalline silicon (p-Si); in the case of the apartment block, hetero-junction, amorphous silicon thin layer over mono-crystalline bulk (m-Si/a-Si), is employed; then, there is a test facility with three arrays made of thin film, i.e., amorphous/micro-crystalline silicon ( $\mu c/a$ -Si), Cadmium Telluride (CdTe) and Copper Indium di-Selenide (CIS). A brief description of each PV plant follows with examples of the monitoring results.

### 2.4.1 Public school “A” (9 years old)

This PV plant was installed in 2004 on a flat roof of a school in the Turin downtown. The rightly cooled p-Si modules, form a PV field of 19.8 kW<sub>p</sub> with 35° tilt angle. Since 2009 one of the three inverters is out of order (maybe due to outdoor installation) and thus the rated power is downgraded to 13.2 kW<sub>p</sub>. Due to the city centre location, a suitable ARPA station has been selected to obtain real historical data of the solar irradiance. As shown in the Fig. 2.4, despite the absence of evident failure of the analysed part of the PV plant, the energy production was poor, compared with the expected values, resulting in an energy availability around 70%. Further notes are added in the following.

### 2.4.2 Public school “B” (9 years old)

This PV plant with a tilt angle of  $20^\circ$  is partially integrated on the roof of a school very close to the previous one. The PV module technology and the power rating are the same. Also in this case the ARPA station does not change. This PV plant presented a failure in a module, a little shade due to a roof profile modification, made after the PV system installation, and some insulation problems of the DC cables. As expected, the energy production was poor with  $R_p \approx 50\%$  and an energy availability of 78%.

### 2.4.3 Public school “C” (7 years old)

This PV system is installed on the ground, with a tilt angle of  $35^\circ$ . The total PV field rates for  $11.78 \text{ kW}_p$ , formed by p-Si modules. The school is in the urban area of Turin, as well as the chosen ARPA station. In this case, the main problem is a residual current device with a low threshold, which causes the PV system to disconnect from the grid with rainy weather conditions (Fig. 2.5). Also in this case the inverters are located outdoor. The energy production can be classified as mean with  $R_p \approx 65\%$  and an energy availability of 81%.

### 2.4.4 Public school “D” (7 years old)

This PV system is integrated on a laboratory roof (poor cooling) in a school for agriculture, with a tilt angle of  $30^\circ$ . The PV power rating is  $8.99 \text{ kW}_p$ , with the same technology of PV modules and inverters as in the previous system. Contrary, the inverters are installed in a proper room. The school is in the countryside of the Turin Province, so a close ARPA station is selected. The behaviour of this PV plant in Fig. ?? is sufficiently in agreement with the energy prediction:  $R_p \approx 73\%$  and  $A_E \approx 95\%$ .

### 2.4.5 Public school “E” (8 years old)

This p-Si plant is formed by a sub-field of  $8.88 \text{ kW}_p$  placed on a flat roof, with a tilt angle of  $30^\circ$ , and another of  $8.88 \text{ kW}_p$  mounted on six double-axis sun trackers. Since 2009 one inverter does not operate, so the PV power rating of

the last sub-field accounts for 5.92 kW<sub>p</sub>. The school is located in the suburbs of Turin, thus another ARPA station is chosen. This PV plant is subject to shade from near obstacles (as e.g. trees), mainly in the sun-tracking part. Moreover, a sun-tracker has lost its right alignment. Actually, the behaviour is poor, with availability  $A_E = 77\%$  for the fixed sub-field and  $A_E = 62\%$  for the sun-tracking one (Fig. 2.6), with  $R_p \approx 55\%$  and 41%, respectively.

### 2.4.6 Factory plant (4 years old)

The PV system, partially integrated on the roof of a factory, is formed by two equal sub-fields: the first one, 125.6 kW<sub>p</sub>, labelled as “1”, is made of m-Si modules; the other one, named as “2”, is formed by p-Si modules. Both sub-fields share the same 30° tilted roof. The factory location is in the suburbs of Turin, so the same ARPA station as for the public school “E” is selected. As illustrated in Fig. 2.7, this plant has very satisfying behaviour, at least for the m-Si array, showing an availability > 99% and  $R_p = 80\%$ , while the sub-field with p-Si modules shows an availability of 95%, with an energy production classified as sufficient ( $R_p = 74\%$ ).

### 2.4.7 Apartment block (3 years old)

This small PV system is presented as an example of residential installation, in a small town, considered as suburban environment and with the hetero-junction PV module technology (m-Si/a-Si). The power rating is 2.53 kW<sub>p</sub> by a single string equipped with minimum number of protections. The PV modules are partially integrated (proper cooling) on a 28° tilted roof. This system shows an excellent behaviour (Fig. 2.8), with the highest performance ratio ( $R_p = 82-83\%$ ) and an energy availability > 99%.

### 2.4.8 Climbing Centre (6 years old)

The PV system installed over a climbing centre in the city of Turin is an actual BIPV system, peculiar for the architectural solution and the solar cell technology. The PV modules are made of three glass layers which laminate m-Si cells and

are totally integrated in the building, creating a rooftop transparent to sunlight. The power rating is  $10.9 \text{ kW}_p$  and the tilt angle is  $30^\circ$ . This system is affected by heavy shade and its energy production is poor,  $R_p = 44$

### 2.4.9 Industrial Test Laboratory (3 years old)

The last three PV systems are small arrays installed over the same covering with  $35^\circ$  tilt angle. They are made of thin film PV modules: in particular, they are  $\mu\text{c/a-Si}$ , CdTe and CIS modules. The power ratings are  $2.1 \text{ kW}_p$ ,  $2.18 \text{ kW}_p$  and  $2.2 \text{ kW}_p$ , respectively, with identical inverters. The array with  $\mu\text{c/a-Si}$  modules can be considered good, since its  $R_p = 78\%$  and the energy availability  $A_E = 97\%$  (Fig. 2.9). The worst production belongs to the CdTe one (Fig. 2.10) with a mean energy production ( $R_p = 69\%$ ), resulting in a negative deviation of  $-12.2\%$ , but it must be stressed that an amount of  $6.5\%$  is due to tolerance I-V mismatch, as it results in Fig. 2.12 from our experimental measurements of I-V characteristics (according to [43] instead of [44]). Hence, the energy availability does not achieve the  $95\%$  threshold ( $A_E = 94\%$ ). The CIS system shows the best behaviour with a  $R_p = 82\%$  and an availability  $> 99\%$  (Fig. 2.11). The results of the

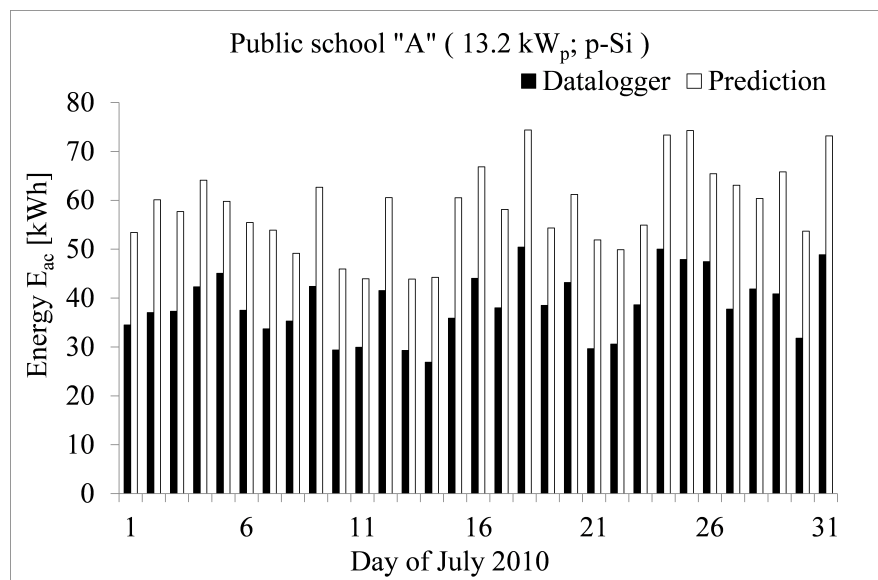


Figure 2.4: Measurements vs. simulations (school A).

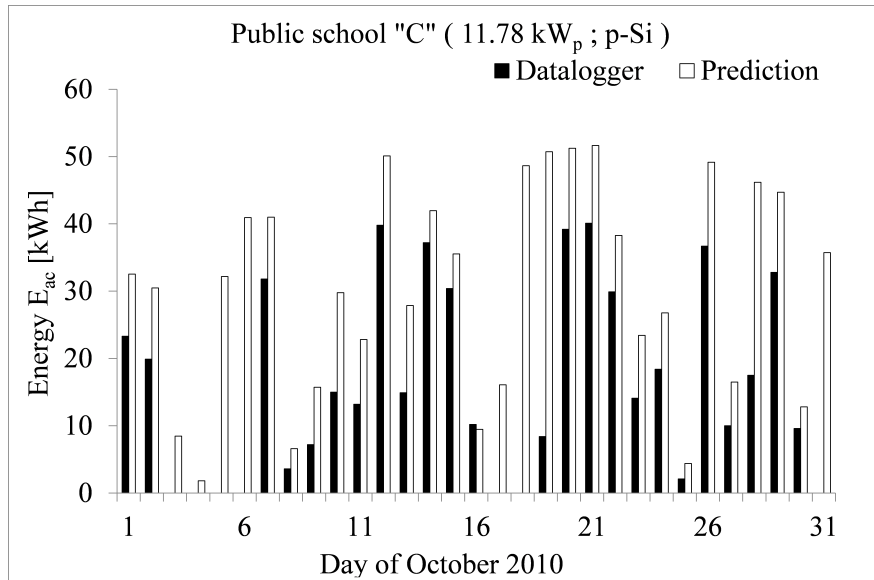


Figure 2.5: Measurements vs. simulations (school C).

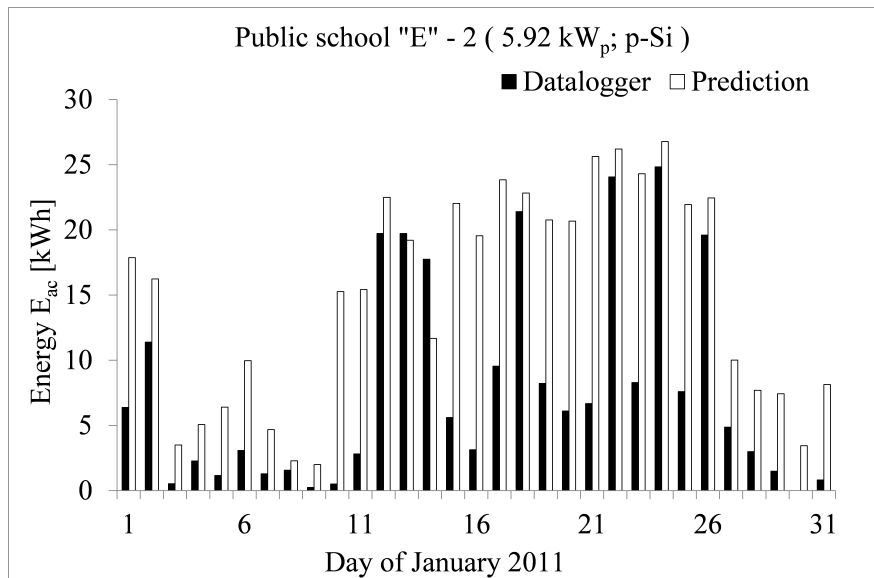


Figure 2.6: Measurements vs. simulations (school E-2).

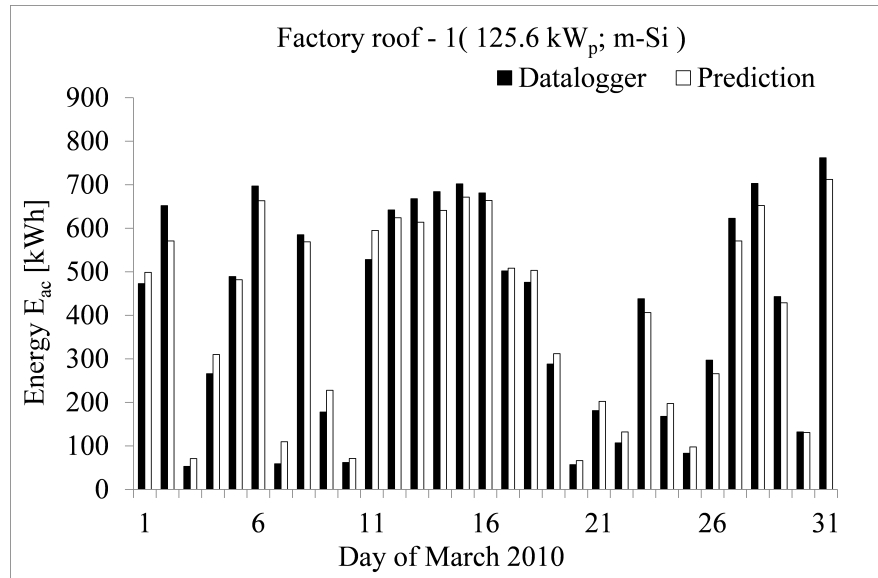


Figure 2.7: Measurements vs. simulations (industrial user-1).

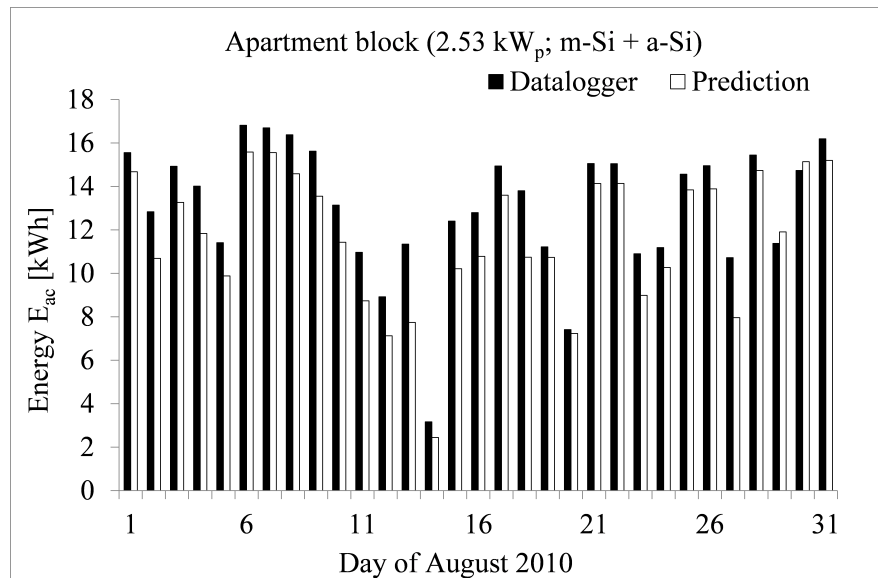


Figure 2.8: Measurements vs. simulations (Apartment block).

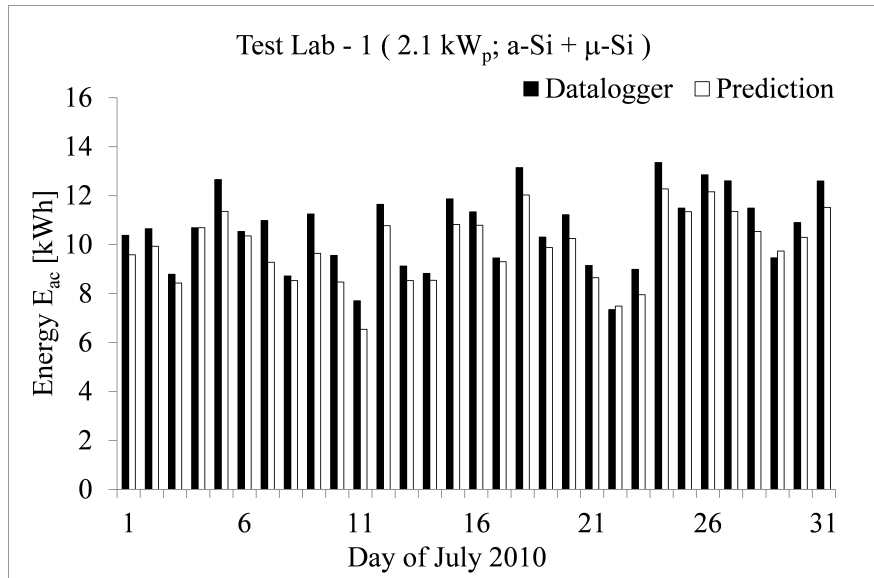


Figure 2.9: Measurements vs. simulations (Test Lab-1).

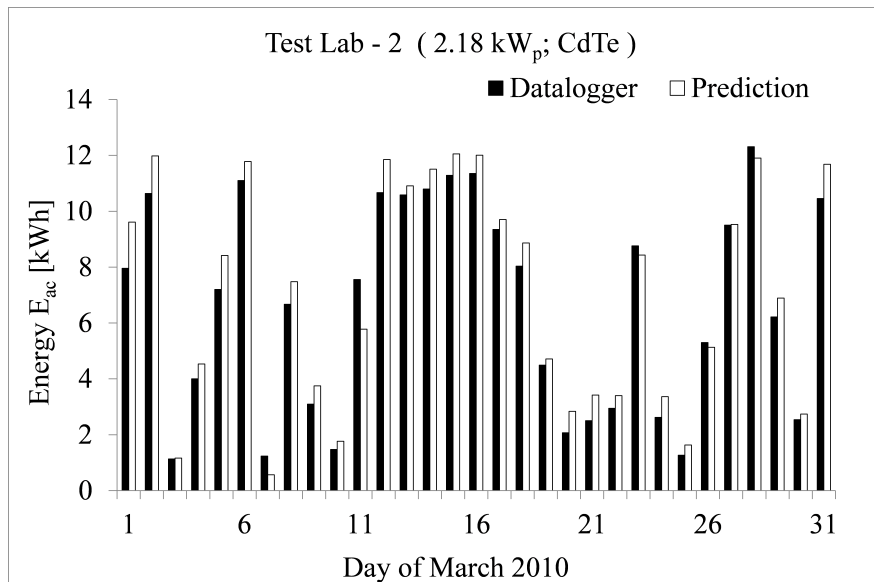


Figure 2.10: Measurements vs. simulations (Test Lab-2).

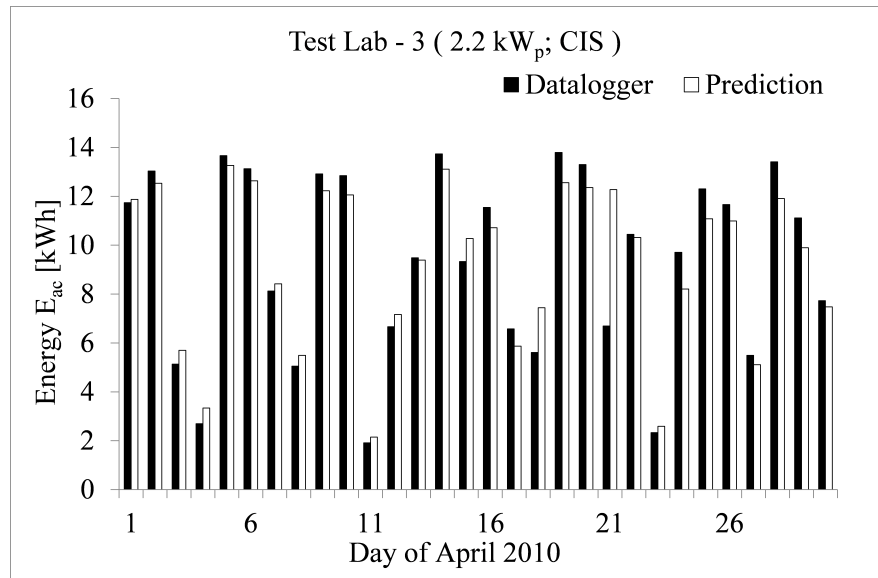


Figure 2.11: Measurements vs. simulations (Test Lab-3).

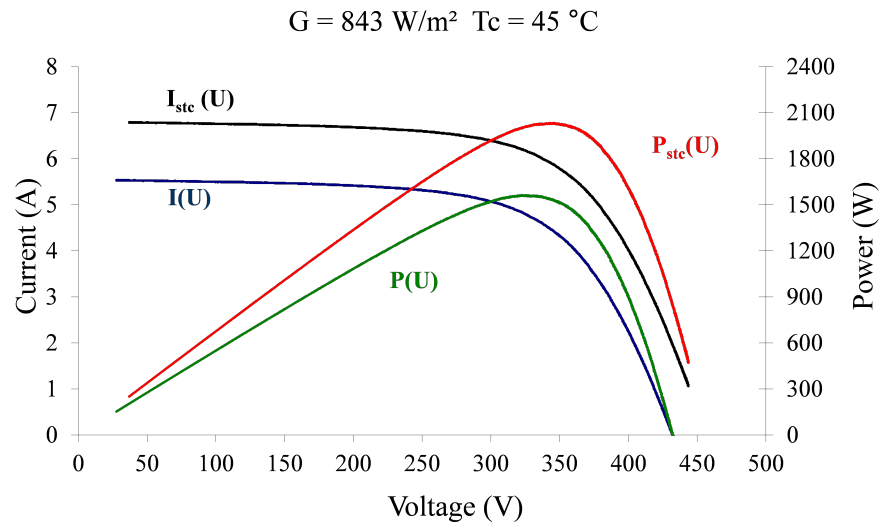


Figure 2.12: Measurements of  $I(V)$  and  $P(V)$  curves at actual conditions and at STC conditions (Test Lab-2).



monitoring activity are summed up in the table in Fig. 2.13.

## 2.5 Discussion about the Analysis Results

If the focus is on the PV plants with poor performance, which can help to improve the future PV systems, the attention is on the public school E. By comparing the performance of mobile vs. fixed PV arrays, the corresponding measured gain is remarkably less than the predicted one. That is due to:

- considerable impact, during the movement, of the shading generated by obstacles such as close trees and the other sun-trackers;
- the need of maintenance of electric motors in the sun-trackers, for avoiding misalignments.

In order to explain these two different drawbacks inherent into sun-trackers, some figures showing the daily power profiles can be included. With respect to the same clear-sky day in winter, Fig. 2.14 shows the typical evolution in a South-oriented fixed system without obstructions: the generated powers from two successive strings of the same inverter are practically identical. If we compare this result with the corresponding evolution of two strings belonging to different sun-trackers Fig. 2.15, it is clear that the mobile PV system achieves gains both at the local noon and in the morning/evening period. However, one can note the misalignment of one string (curve in blue colour) vs. the other one (curve in red colour): maybe the sun-tracker motor cannot go back to the starting position towards East at the end of the sunlight hours and in the next day the string is affected by a position delay. Furthermore, also the right-moving string is not working properly because it is subject to the shade of a surrounding tree in the afternoon with a shading efficiency  $\eta_{shade} \approx 86\%$  (Fig. 2.16). By continuing the analysis of the poor PV systems, all the oldest plants (A, B and E) were designed with a great degree of protections due to a pessimistic approach, typical when a new technology is employed. The use of fuses and blocking diodes, also for a few parallel connected strings, is a way of protecting plants which requires a timely substitution of the devices in order to preserve the reliability, but often the service

	Public School "A"	Public School "B"	Public School "C"	Public School "D"	Public School "E" - 1
$P_{rated}$ [kW]	13.20	19.80	11.78	8.99	8.88
Technology	p-Si	p-Si	p-Si	p-Si	p-Si
Tilt ( $^{\circ}$ )	35	20	35	30	30
Azimuth ( $^{\circ}$ )	30	30	30	0	29
ARPA station	urban	urban	urban	country	urban
Period	Apr 2010 - Feb 2011	Mar 2010 - Feb 2011	Sep 2010 - May 2011	May 2010 - Apr 2011	Dec 2010 - Sep 2011
$E_{ac}$ [kWh]	5526	9506	6635	8465	5819
$Y_r$ [tperiod $^{-1}$ ]	1151	1442	868	1286	1336
$Y_f$ [tperiod $^{-1}$ ]	507	720	563	942	729
$R_p$	0.44	0.50	0.65	0.73	0.55
$A_E$	70%	78%	81%	95%	77%
Rank	poor	poor	mean	sufficient	poor

	Public School "E" - 2	Factory roof - 1	Factory roof - 2	Apartment block	Apartment block
$P_{rated}$ [kW]	5.92	125.60	125.74	2.53	2.53
Technology	p-Si	m-Si	p-Si	m-Si + a-Si	m-Si + a-Si
Tilt ( $^{\circ}$ )	Double axis sun tracking	30	30	28	28
Azimuth ( $^{\circ}$ )		7	7	5	5
ARPA station	urban	urban	urban	suburb	suburb
Period	Dec 2010 - Sep 2011	Mar 2010 - Feb 2011	Mar 2010 - Feb 2011	Apr 2010 - Mar 2011	Jan - Dec 2011
$E_{ac}$ [kWh]	4261	147587	136372	3142	3515
$Y_r$ [tperiod $^{-1}$ ]	1745	1462	1462	1493	1695
$Y_f$ [tperiod $^{-1}$ ]	720	1175	1085	1242	1389
$R_p$	0.41	0.80	0.74	0.83	0.82
$A_E$	62%	99%	95%	99%	99%
Rank	poor	excellent	sufficient	excellent	excellent

	Climbing Centre	Test Lab - 1	Test Lab - 2	Test Lab - 3
$P_{rated}$ [kW]	10.90	2.10	2.18	2.20
Technology	m-Si	a-Si + $\mu$ -Si	CdTe	CIS
Tilt ( $^{\circ}$ )	30	35	35	35
Azimuth ( $^{\circ}$ )	5	20	20	20
ARPA station	urban	country	country	country
Period	May 2010 - Mar 2011	Feb - Sep 2011	Feb - Sep 2011	Feb - Sep 2011
$E_{ac}$ [kWh]	5526	1980	1805	2174
$Y_r$ [tperiod $^{-1}$ ]	1151	1205	1205	1205
$Y_f$ [tperiod $^{-1}$ ]	507	943	830	988
$R_p$	0.44	0.78	0.69	0.82
$A_E$	88%	97%	94%	99%
Rank	poor	good	mean	excellent

Figure 2.13: PV System Specifications and Comprehensive Performance Parameters.

personnel is expensive and a portion of the plant remains out of order. Then, examining the public schools C and D, which are equipped with the same components in terms of PV modules and inverters, it is worth noting that system C is worse than system D. The main reason is the different type of installation for the inverters, i.e., in the first case the devices are placed outdoor, whereas in the second case the devices are located in a proper room. In fact, the outdoor installation causes an increment of the leakage current towards ground, usual in a transformer-less inverter, when the moisture is high as in rainy days (Fig. 2.5). Consequently, the connection of a very sensitive residual current device, as a protection against indirect contacts, means a high probability of tripping when the weather is overcast. A further poor PV system is the “climbing centre” plant, characterized by huge shade projected by an adjacent higher wall: the best choice of the designer should be to avoid the installation of array 1, rather than to split the PV modules into three different arrays to mitigate the shading effect. Actually, it is evident from the power profiles that only one inverter (array 3, the smallest in Fig. 2.17) is not affected by the heavy worsening in the performance: the weighted average shading efficiency, in particular, can be estimated  $\eta_{shade} \approx 78\%$ , resulting from the individual values of the different arrays equal to 63%, 82% and 91%. Furthermore, dirt and soiling [37], usual in a big city as Turin (about 1 million of inhabitants), are sources of additional losses. An interesting case study is the factory roof, in which the PV plant ( $250 \text{ kW}_p$ ) is divided into two equal parts, one array is equipped with m-Si modules and the other one with p-Si modules, while the inverters are identical. The m-Si performance is much better than the p-Si one: the reasons can be identified in both the higher spectral absorption typical of the single-crystal lattice (close to sunrise/sunset) and the different availability of the inverters, usual when the electronic components are undersized due to wide tolerance in their parameters. Also in the test facility, the different availability of the three equal inverters (same manufacturer and same model) can be generated by components which are undersized in some operating conditions. These weak points produce less hours of operation for the energy conversion. The  $2.5 \text{ kW}_p$  system, placed on the roof of the apartment block with negligible shading, is characterized by very efficient components, suitably cooled, that permit the fulfilment of the predicted performance (Fig. 2.8). In this case

the simple model for energy production (with assumption of 100% availability) exhibits noticeable accordance with the data-logger readings. Similar notes are valid for the CIS array within the test facility.

In conclusion, this achieved goal for the energy production is due to:

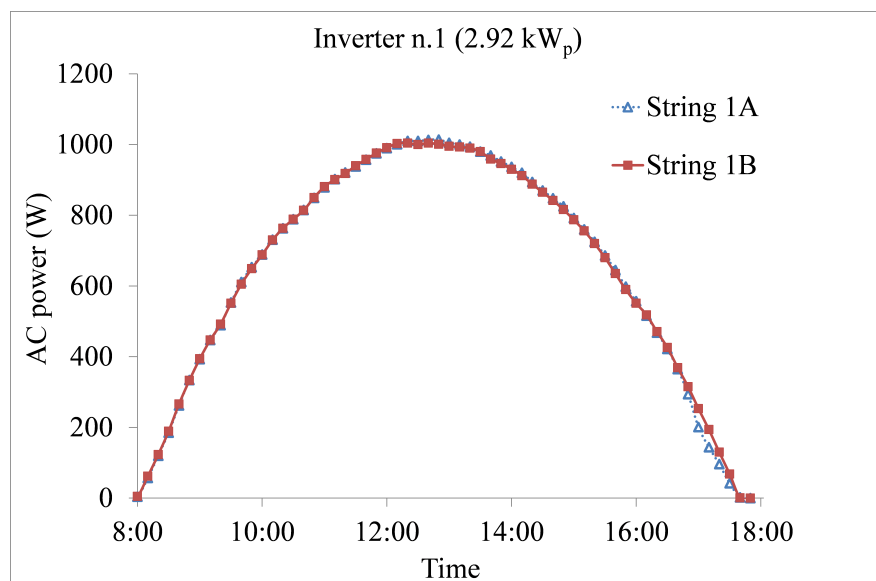


Figure 2.14: Daily power profiles of two fixed strings.

- the natural convection on the PV modules (some centimetres of air gap between tiles and PV devices);
- the transformer-less configuration of the grid-connected inverter;
- the low temperature in the room of the inverter;
- the combined adoption of solar cables and minimum number of protection components.

All these remarks have been included in detail in the guidelines for the design, installation and maintenance of PV systems produced at the end of the PERSIL project.

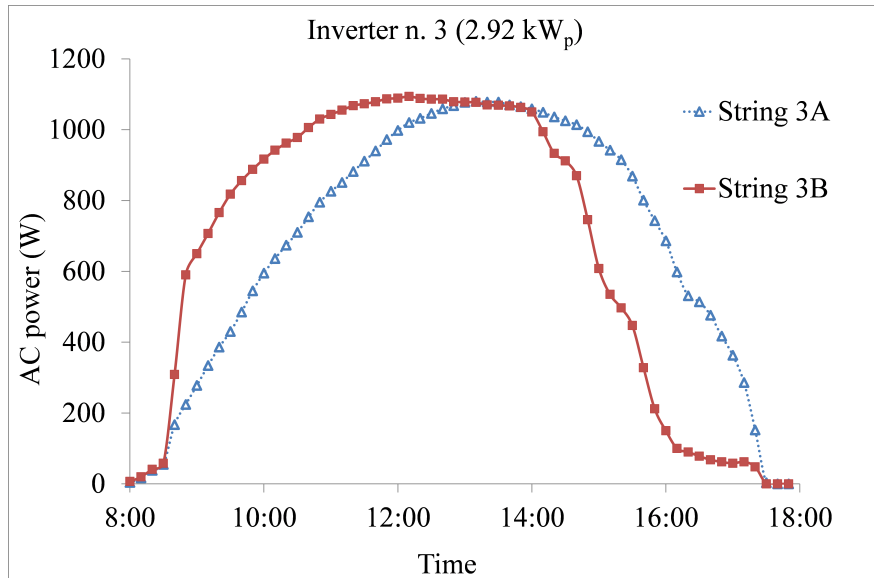


Figure 2.15: Misalignment in a sun-tracker (string 3A).

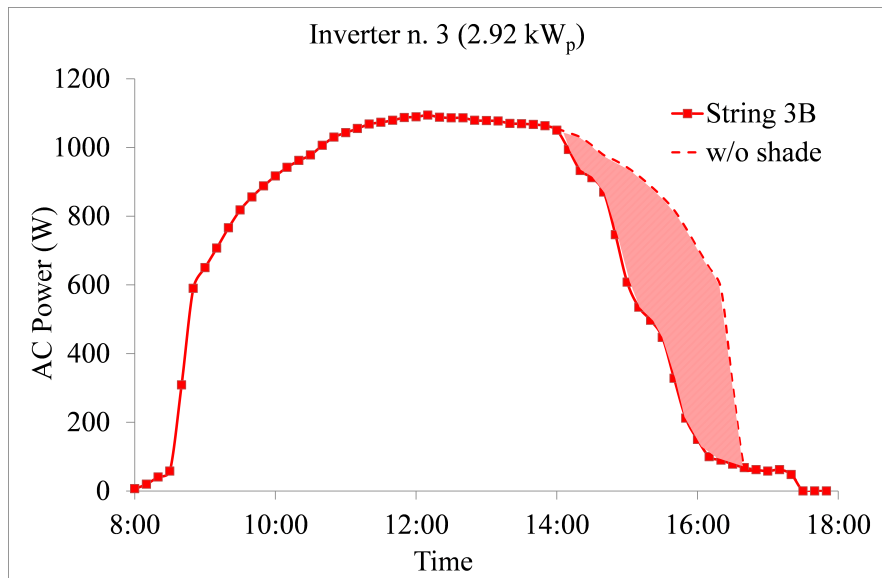


Figure 2.16: Shading effect impact in a sun-tracker (string 3B).

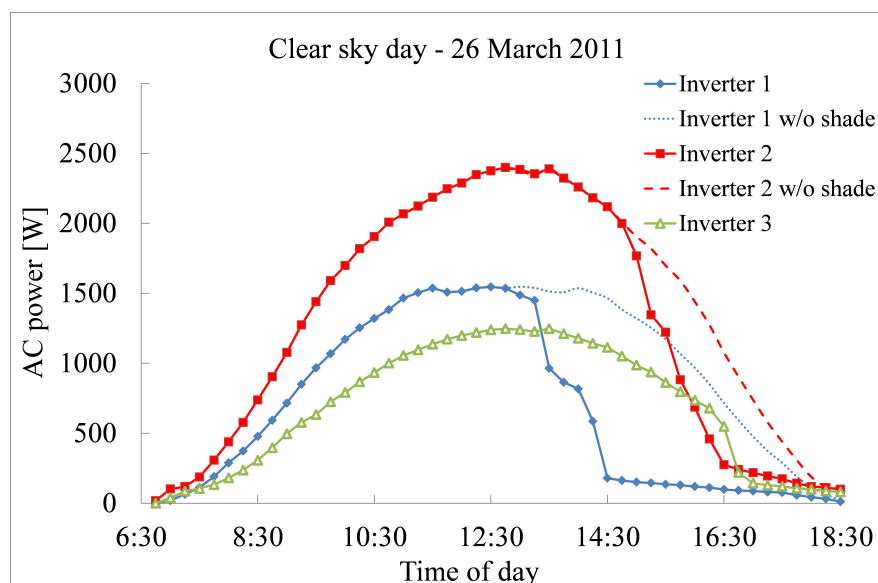


Figure 2.17: Evolution of the shade on the climbing centre.

## 2.6 Concluding remarks

This chapter includes the 1-year monitoring results of thirteen PV systems in grid connection. The work was an important part of the European Project PER-SIL, joint collaboration between public and private administrations in Italy and France.

A two-year analysis of monthly irradiations puts into evidence the role of an accurate and local measurement by pyranometers in the framework of the current climate changes. Actually, mutual distances between meteorological station and PV plant higher than 5-10 km and/or the lack of the radiation data for the year under study can cause noticeable errors in the calculation of the performance ratio.

The consequent experimental results in terms of operational parameters show that three PV plants behave in excellent manner ( $PR = 0.80-0.83$ ), whereas five PV plants exhibit poor energy production ( $PR = 0.41-0.55$ , mainly owing to loss of availability) and the remainder has average behaviour.

The simple model, without the assessment of the energy availability, exhibits adequate accuracy for the productivity, if the PV system is equipped with efficient

---

and reliable components, suitably cooled and oversized. Moreover, the presented improvement of the model proves that the energy availability for old PV plants is less than 95%, while more recent PV plants show values up to 99%. When a new plant is characterized by low availability, as in the case of the factory p-Si plant or the CdTe one, in which the inverters are the same of the remaining part (excellent) of the PV systems, the reason can be found in the components with undersize consequent to wide tolerance in their parameters.

The study also highlight that the worst case in terms of energy availability is represented by the sun-tracking PV plant, due to the complete lack of mechanical maintenance.

Finally, the guidelines produced, and here not reported, help to maximize the energy availability and can be easily extended to the other Countries that accept the IEC or IEEE Standards.

